International Journal of Composite Materials 2021, 11(2): 23-35
DOI: 10.5923/j.cmaterials.20211102.01

Ballistic Impact Performance of Triangular Corrugated Core Sandwich Composite Armor

Shah Alam*, Samhith Shakar

Department of Mechanical & Industrial Engineering, Texas A&M University-Kingsville, Kingsville, TX, USA

Abstract This study focused on the design, modelling and the analysis of the dynamic response of sandwich composite armor system, constructed with kevlar 29/phenolic matrix, carbon fiber/epoxy (T300 6k/ Epon 862) and carbon fiber/epoxy (T300 6k/ Epon 862, with 4% carbon nanotube) as top and bottom skins. The core of the sandwich composite armor was made of triangular corrugated aluminum structure filled with prismatic silicon carbide. The triangular corrugated core was used to change the direction of bullet. The skin thickness, material composition, impact velocity etc., was varied to get their influence on the impact resistance of the armor system. The sandwich structure typically consisted of front plate, core and backing plate, which was impacted at different velocities starting at 1400 m/s to 1700 m/s, where complete armor penetration was noticed. From the dynamic analysis, the residual velocity and energy absorption capacity were obtained and the energy absorption capacity for various configurations were compared. The results of all models with 2mm, 3mm and 4mm skin thickness revealed increased energy absorption of the sandwich armors with carbon fiber/epoxy (T300 6k/ Epon 862, with 4% carbon nanotube) as skins and with kevlar 29/phenolic matrix as skins the sandwich armor yielded the least energy absorption. The sandwich composite armor model used in this research was unique in-terms of skin composition, combination of materials, geometry and assembly. Due to limitations of manufacturing and testing facilities of the sandwich composite armor, a kevlar/epoxy laminate finite element model was validated with the experimental test results found in the literature. The deviation of the results was noticed, and the reasons of deviation were discussed.

Keywords Composite Armor, Ballistic Impact, Finite Element Analysis

1. Introduction

Human's protection has been an important issue since the beginning of creation. Throughout the recorded history, there have been various types of materials that are utilized as protection garments from injury such as in battle and other dangerous situations [1]. There are several armor solutions for effective ballistic protection by using advanced alloys, ceramics and composite materials. One of these important solutions is the sandwich structure of alumina ceramics together with Kevlar reinforced composite materials. Even though it requires high technology for the production of alumina and it is not easy to configure it for the complex geometries, low density, good thermal shock resistance and higher hardness, kit demonstrates a good candidacy for armor solution [2].

A deeper study in the stacking and structuring of composite armor has led to the experimental investigation of the blast responses of fiber metal laminates (FMLs) and gradient aluminum sandwich panels with FML skins. A parametric investigation was carried out by considering five different core layer arrangements with different cell geometries. In terms of FML face sheets and gradient honeycomb core, the various modes of deformations and failure were obtained in the experiment. It was also found that the impact resistance depends not only on the cell geometry and arrangements of core layers, but also related to the magnitude and rate of target loading which leads to different deformation/failure mechanism of panels [3].

The research in the field of exotic carbon allotropes has introduced a material called 'Graphene', which is found to have the potential of revolutionizing the concept of body armors. Graphene is made up of a single layer of graphite, which is composed of a hexagonal lattice of carbon atoms. With the exhibition of extreme strength and tremendously lightweight characteristics has made graphene a special interest for militaries. The excellent properties of durability and fixability of the material has proven that it can be very robust and aiding to troops, who endure extreme conditions. With the usage of graphene in armor system, it is found that the strength is increased significantly with extreme reduction in weight [4].

The safety of human beings in battlefield is emphasized extensively. The design of body armor is carried out having safety of the user and unrestricted mobility in mind. Over the

* Corresponding author:
alam1610@gmail.com (Shah Alam)
Received: Jul. 11, 2021; Accepted: Aug. 23, 2021; Published: Sep. 10, 2021
Published online at http://journal.sapub.org/cmaterials

past decades there has been a pressing need for specific energy absorption capacity, which has paved way for the development and improvement of body armor made of high strength fabrics and ceramic materials, which has proven to be lightweight, along with better performance compared to their metal predecessors [5].

With the introduction of carbon fibers and other fabric material, has paved way for a new class of body armors. The usage of carbon fibers and other composites have revolutions the concept of body armors with significant improvement in performance and considerable reduction in weight. Extensive research in the field has reported a facile method to study and investigate the effects caused by the stacking sequence of layers making up the hybrid composite materials in terms of ballistic energy absorption by performing the ballistic test at high velocity impact conditions. A series of specimen made of kevlar, carbon glass woven fabrics and resin were experimentally instigated under high velocity impact conditions with varied stacking sequence. The post analysis of the ballistic impact revealed the energy absorption; accordingly, the ballistic impact resistance of the material was found by the conduction of the test [6].

In a study kevlar/filled epoxy matrix is investigated for its ballistic impact behavior. To increase impact performance with significant reduction in weight, three different fillers, nano clay, nanocalite and nanocarbon were used in the composite armor. Along with the filler material the nanocarbon were dispersed in a 0.5%, 1% and 2% weight ratio relating to the epoxy matrix. The results from ballistic impact test discussed about the damage perforation [7].

An investigation for improved ballistic impact response is carried out on alumina-ultra high molecular weight polyethylene (UHMWPE). The UHMWPE composites are investigated under different relative concentrations of alumina. The post test results revealed that the depth of penetration (DOP) in a medium density fiberboard (MDF) bulkhead protected by a disc of the composite decreased considerably with higher concentration of alumina in the composites. The composites with 80%, 85% and 95% alumina showed trans angular, interangular and ductile fracture mechanism, which was analyzed using images of scanning electron microscopy. Among all specimens of different relative concentrations of alumina, the composition A90 (90% alumina and 10% UHMWPE) was the one preferred with its performance in terms of weight and penetration depth [8].

In a study [9], a glass fabric/epoxy laminate is considered, which was subjected to low velocity impacts at different energy levels. This low-velocity impact conditions were modelled and analyzed implementing finite element modelling using LS-DYNA. The material under consideration was defined using solid finite elements along with orthotropic failure criteria. For specifying the delamination mechanism, a stress-based contact failure between the plies was adopted. The study found that there was a good correlation with experimental data and numerical simulation in terms of material damage and energy curves.

The constituent materials of a composite armor are categorized into ceramics and fiber reinforced polymer (FPR). A detailed examination of these constituent materials was described. At first the constituent materials were examined individually and was followed by comparison of the individual result with other constituent materials considered. A close study was conducted to review the characteristic change with various combinations of constituent material, which had helped them study different configuration of armor system. They also reviewed and considered the effect of bullet geometry and composition. The study helped them to arrive at optimized combination of constituent materials and they also reviewed the futuristic potential and versatility of composite armor [10].

A composite armor system with Aluminum ceramic with sandwiched between kevlar plates was studied [11]. The Aluminum ceramic chosen had excellent properties of hardness, thermal shock resistance and corrosion resistance. The multilayered composite structure was tested at low velocity impact testing set up and subsequent damage analysis was carried out. The study helped to arrive at minimum impact energy level and its fragment velocity equivalent. The FE analysis carried out using Ansys/Autodyne, verified the data obtained from testing. The FE analysis helped in concluding that the multilayered composite structure under investigation provides protection against impact energy of 25 caliber machine gun bullet fired from 50 meters away or impact energy of 22 caliber bullet with an impact velocity of 225 m/s from 200 meters away.

A good armor needs to have good impact resistance and high strength to weight ratio. This makes kevlar fibers the most suitable option for usage as reinforcement in military and civil protection armor system. In this study, kevlar/filled epoxy matrix was investigated for its ballistic impact behavior. To increase impact performance with significant reduction in weight, three different fillers, nano clay, nanocalite and nanocarbon were used in the composite armor. Along with the filler material the nanocarbon were dispersed in a 0.5%, 1% and 2% weight ratio relating to the epoxy matrix. The results from ballistic impact test discussed about the damage perforation [12].

A detailed study was carried out to review the effects of projectile penetration into ceramic composite armors. The standard 30 mm projectile was replaced with a projectile with toughened ceramic node. The ceramic nose was impacted on the ceramic/A3 steel plate to study the performance of penetration using impact dynamics theory. The projectile penetration was analyzed and compared with other nose structure and composition using DOP method. The analysis revealed difference in aperture, depth of preformation and also residual mass of the projectile due to penetration. Furthermore, a numerical simulation using Finite element methods was constructed using ANSYS/LS-DYNA. Using the simulation results, the projectile penetration was analyzed in terms of residual mass of the projectile core. The study concludes that the ceramic nose had a great effect on projectile core protection [13].

With the demonstration of excellent properties of strength and extreme lightweight has enabled Graphene to be an appealing candidate in the field of armors. A study of high velocity impact at 2-6 km/s, based on a series of specimens were considered. It was witnessed that the crack formation was preferentially in zigzag direction, when observed from tensile deformation standpoint. The mechanism eventually has an influence on the penetration and growth of crack. The study shows that the circular shape graphene possesses the best impact resistance. It was also found that higher kinetic energy results in a greater number of cracks. The study has furthermore strengthened, the fundamental understanding in terms of deformation mechanism of monolayer graphene subjected to high velocity impacts. This fundamental understanding has helped in arriving at solutions for engineering challenges related to the future applications of graphene in armors and protective shielding of spacecraft from orbital debris [14].

In a study, a detailed review of multi layered composite armor behavior and damage formation mechanism with an intermediate or center layer made of different material was considered. The inter layers considered in this study is rubber, Teflon and aluminum foam sandwiched between a ceramic front plate and composite back plate. The series of specimen with different inter layer composition are tested under low velocity impact condition and analyzed using numerical methods implemented using the non-linear finite element software LS DYNA. The results from the numerical studies showed a decrease in the transmission of stress waves to the composite back plate with the usage of Teflon and foam as inter layers. It was also observed that there was an increase in impedance during impact. Furthermore, the study also reviewed the increased in damage formation of the ceramic front face plate, attributed by the decrease in stress wave transmission to the ceramic back face [15].

Engineering failures and challenges in the past led to a sophisticated and tangible solution in terms of the finite element model and analysis. Remarkable events like the return-to-flight preparations following the Colombia accident, paved way to the emergency and emphasis of finite element modelling to predict the threshold of critical damage to various components at extreme conditions. This led to the initiation of an experimental program in view of providing crushing data from impacted ice for use in dynamic condition of finite element models. The continued effort of the program led to the configuration of a drop tower with high-speed capabilities to record force- time histories of ice cylinders at impact velocities up to 100 ft/s. The force time history depended majorly on the internal crystalline structure of the ice, but for velocities of 100 ft/s and above, the ice fractured on impact and demonstrating behavior more analogous to fluid. A closer review also showed that the subsequent force-time history curves turned out to be less dependent on the internal crystalline structure of ice [16].

Multilayer graphene and polyvinyl alcohol (MLG/PVA) films were studied by O'Masta, et al. [17]. The MLG/PVA films were subjected to edge clamped quasi-static and dynamic loading conditions. The specimen under consideration was 85 mm square and 10 µm thick film, which was reinforced by 35% vol of MLG by liquid exfoliation technique. The MLG/PVA films were experimentally compared with other specimens with different composition (pure PVA and aluminum) of equal mass/area. The series of test showed that the young's modulus of MLG/PVA films were twice that of PVA films. It was also noticed that the MLG/PVA films had a low strain rate peak strength which was close to 50% higher than pure PVA films. The MLG/PVA films were compared with Al films which showed that the MLG/PVA films were stiffer and had a relatively high load carrying capacity. Furthermore, the ballistic limit test was conducted, where it was found that the MLG/PVA films was 50% higher than the Al films but the parent PVA films had a higher ballistic resistance, because of their higher ductility in comparison. The prediction of ballistic resistance of the MLG/PVA films was arrive at by implementing member stretching analysis which helped in the understanding of ballistic resistance potential of graphene/PVA composite films [18].

After reviewing all these research papers related composite sandwich armor, the potential and emphasis in the field of sandwich composite armors was realized. Usage of carbon fiber reinforced polymers with carbon nanotubes as skins, has received little research attention and the robust application is unexplored. The literature also conveyed the importance of triangular corrugated core structure integrated with ceramics in achieving better results of impact resistance. A combination of these components and their configuration, leads to a whole new avenue of research. The triangular corrugated core filed with ceramic is new in this research. The triangular core will deviate the bullet impact direction and reduce the bullet speed.

2. Methodology

Composites exhibit anisotropy in mechanical properties meaning their values are directionally dependent. The damage in laminated composites results from matrix cracking, fiber matrix debonding, fiber fracture and delamination. The onset of damage causes a reduction in load carrying capacity if the plates and numerically this is computed by estimating the corresponding reduction of the stiffness matrix components. Classical laminate/composite analysis can then calculate the overall resulting mechanical properties of the layers, post stiffness reduction.

2.1. Finite Element Analysis

The study of energy absorption modes and failure pattern observed in armor first prompt the use of numerical codes that predict the ballistic performance. Similar to analytical modeling of an impact problem, FEA codes can also be used to combine the various energy dissipation modes in one analysis and predict the ballistic resistance and impact worthiness of armor. This method is far more effective

than actual testing, as making variations in design is easy and time effective. Failure modes and deformations from FEA also can be visually inspected to compare accuracy with experimental results. This comparison is a necessary validation step as accuracy of results from FEA is variable since there are no standards to the way FEA is conducted.

The FE models are developed in the commercial software Abaqus/Explicit. It involves the geometric modelling, defining of material model, assigning of properties, assembly of components, step creation, creating interaction, specifying boundary conditions, assigning loads and meshing of parts, etc. In the rest of this section, the details of each component in the FE model is explained.

2.2. Skins

The top and bottom skins are created with a dimension of (120 x 120 x 2 mm). The composite skin is divided into four individual ply of thickness 0.5 mm each. The component is modelled as continuum shell. A circular face is constructed on the face plane of the skin, for assigning a denser mesh inside the circular region.

2.3. Triangular Corrugated Aluminum Core

Corrugated aluminum core is created as shown in Figure 1. With each cell having a geometric profile of equilateral triangle, with a side length of 22mm, shell thickness of 3.2mm and an extruded length of 120mm. The part is modelled as shell element and assigned with the material properties of Aluminum 7039.

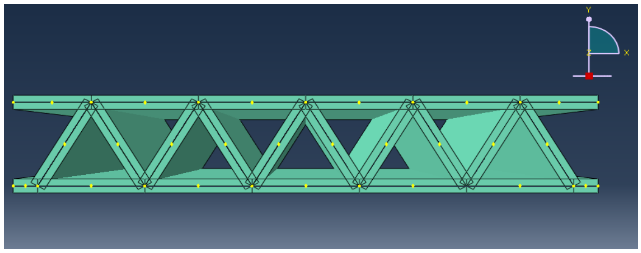

Figure 1. Triangular corrugated core

2.4. Centerpiece

The centerpiece has the dimensions of an equilateral triangle with a side length of 16.45 mm and a height of 14.24 mm. This triangular profile is extruded in z direction to a length of 120mm. The centerpiece is modelled as solid element and is assigned with material properties of Silicon carbide.

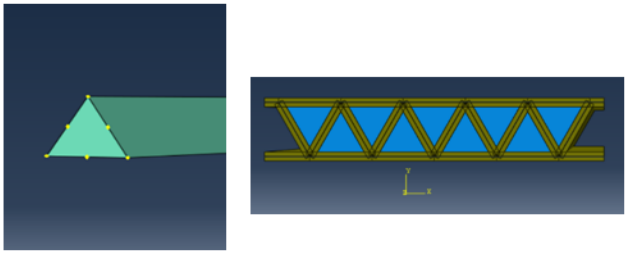

Figure 2. Centerpiece (left) and full assembly of centerpiece inserted into the corrugated structure

These blocks are later inserted and accommodated precisely in the spaces of the corrugated structure, which together makes up the core of the sandwich composite armor (Figure 2).

2.5. Projectile

The projectile considered in this study is a 7.62 mm APM2 projectile. Only the steel core is modeled with the assumption that the brass jacket will be stripped off and has no influence during the impact process. The projectile is meshed with eight-node hexahedral element C3D8R. Mesh sensitivity was investigated by varying the element size. The final optimized mesh is used in the analysis.

2.6. Assembly

The assembly (Figure 3) of the sandwich composite armor has the top skin and bottom skin sandwiching with corrugated aluminum core filled with prismatic ceramics. The projectile is separated by a distance of 2mm from the top face of the sandwich structure to initiate impact.

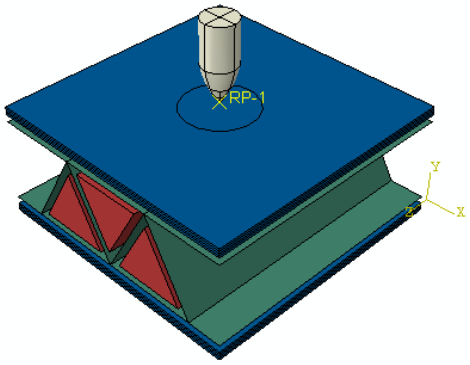

Figure 3. Sandwich composite armor assembly

2.7. Mesh Convergence

It is important to use an appropriate mesh size for obtaining reasonable results with optimum usage of computer resources. The choice of mesh size might have a slight discrepancy in the output results. A fine mesh might increase the number of element level calculation and increase the computational cost but increase accuracy of the results. It is a common fact that refinement of mesh yields better results for most simulations. Mesh sensitivity was investigated by varying the element size and the final optimized mesh is used in the analysis.

2.8. Material Properties

The top and bottom skin used in the sandwich composite armor has the same material composition as well as relative thickness. The composite materials used is varied in different simulation to study the influence of materials and other changes in behavior. The materials and their properties used in this study are Kevlar29/epoxy [20], T300 Epon 862, T300 6k [21,22], Epon 862 with 4% Carbon Nanotube [23], Al7039 [24,25], Sic [26] and steel [27]. The fracture energies

are collected from for FRP [24] and FRP with carbon nanotube [21].

2.9. Material Model Failure Criteria

In dynamic analysis, it is important to choose the appropriate failure criteria for the materials to include damage and element deletion. It is found that, composite materials when modelled with progressive damage criteria yield better results. The top and bottom skins, which are essentially composite materials are modelled using Hashin damage criterion. The centerpieces made of silicon carbide which are brittle materials is modelled using Drucker-Prager failure criterion. The corrugated triangular core made of aluminum is modelled using ductile damage criterion and the projectile being made of steel is modelled using ductile damage criterion.

2.9.1. Progressive Damage Modelling

A material failure is attributed with complete loss of load carrying capacity of which is a direct consequence of progressive degradation of material stiffness. The progressive damage is a combination of damage initiation and damage evolution [27].

2.9.1.1. Damage Initiation

The damage initiation defines the point at which initiation of degradation of material stiffness is seen and the damage evolution defines the post damage initiation behavior of the material. In Abaqus the Hashin damage allows us to specify the damage initiation. The criteria are formed with combined data from fiber tension and compression along with matrix tension and compression damage mechanism involved. The fiber tension, compression, matrix tension and compression equations are listed below [27].

Fiber tensile damage if F_{tf}> 1, where

$$F_{tf} = \left(\frac{\hat{\sigma}_{11}}{X_T}\right)^2 + \alpha\left(\frac{\hat{\tau}_{12}}{S_L}\right)^2$$

Fiber compressive damage if F_{cf}> 1, where

$$F_{cf} = (\frac{\hat{\sigma}_{11}}{X_C})^2 . Ftf = (\frac{\hat{\sigma}_{11}}{X_T})^2 + \alpha(\frac{\hat{\tau}_{12}}{S_L})^2$$

Matrix tensile damage if F_{tm}> 1, where

$$F_{tm} = (\frac{\hat{\sigma}_{22}}{Y_c})^2 + (\frac{\tau_{12}}{S_L})^2$$

Matrix compressive damage if F_{cm}> 1, where

$$F_{cm} = (\frac{\hat{\sigma}_{22}}{2S_T})2 + [(\frac{Y_c}{2S_T})2 - 1].\frac{\hat{\sigma}_{22}}{Y_c} + (\frac{\tau_{12}}{S_L})^2$$

In the above equations, X_T denotes the longitudinal tensile strength; X_C denotes the longitudinal compressive strength; Y_T denotes the transverse tensile strength; Y_C denotes the transverse compressive strength; S_L denotes the longitudinal shear strength; S_T denotes the transverse shear strength; α is a coefficient that determines the contribution of the shear stress to the fiber tensile initiation criterion; and $\hat{\sigma}_{11}, \hat{\sigma}_{22}, \tau_{12}$ are the component stresses.

2.9.1.2. Damage Evolution

In addition to the damage initiation criterion, an energy-based damage evolution criterion was used to characterize the progressive damage of the material. Once the critical energy criterion is satisfied by an element, it will be removed from the simulation.

3. Results and Discussions

Three different sandwich composite armors with different skin composition of Kevlar 29/epoxy, Carbon/Epoxy (T300 6k/ Epon 862) and Carbon/Epoxy (T300 6k/ Epon 862, with 4% carbon nanotube) with a relative skin thickness of 2mm was subjected to impact by the projectile at 1400m/s. The models were analyzed with its characteristic energy absorption by reviewing and comparing the kinetic energy and residual velocity curves.

Figure 4 shows the kinetic energy plot variation with different skin compositions (Kevlar, Carbon Fiber and carbon nanotube) at impact velocity 1400m/s. The variation of kinetic energy among the different skins were very small. The minimum kinetic energy after impact was near zero. Therefore, all models demonstrate no sign of bullet penetration through the armor and all kinetic energy were absorbed by the armor. There are some amounts of kinetic energy lost as dissipation effects. However, sandwich structure with carbon fiber/epoxy (T300 6k/ Epon 862, with 4% carbon nanotube) as skins demonstrated better kinetic absorption characteristics compared to the other models.

Figure 5 shows the comparison of kinetic energy curves of the sandwich armor with skins made of kevlar 29/phenolic matrix, carbon fiber/epoxy (T300 6k/ Epon 862) and carbon fiber/epoxy (T300 6k/ Epon 862, with 4% carbon nanotube) at impact velocity 1600m/s. The curves trace a path very close to each other with a difference in kinetic energy of the smallest order. The sandwich armor with carbon fiber/epoxy (T300 6k/ Epon 862, with 4% carbon nanotube) as skin has demonstrated maximum kinetic energy absorption relative to the other models with different skin material composition in comparison. All three models had bullet penetration through the armor and the bullet had a residual velocity post penetration.

The study is furthered by investigating the impact behavior and kinetic energy absorption of sandwich armors at impact velocities of 1700 m/s. Figure 6 shows the comparison of kinetic energy curves of the sandwich armor with skins made of kevlar 29/phenolic matrix, carbon fiber/epoxy (T300 6k/ Epon 862) and carbon fiber/epoxy (T300 6k/ Epon 862, with 4% carbon nanotube) impacted at a velocity of 1700 m/s. Even at a high impact velocity of 1700 m/s, carbon fiber/epoxy (T300 6k/ Epon 862, with 4% carbon nanotube) has demonstrated higher energy absorption (low kinetic energy), which is determined by looking into the kinetic energy plots. At this particular impact velocities, all three projectiles got penetrated, and the projectile exited with residual velocities.

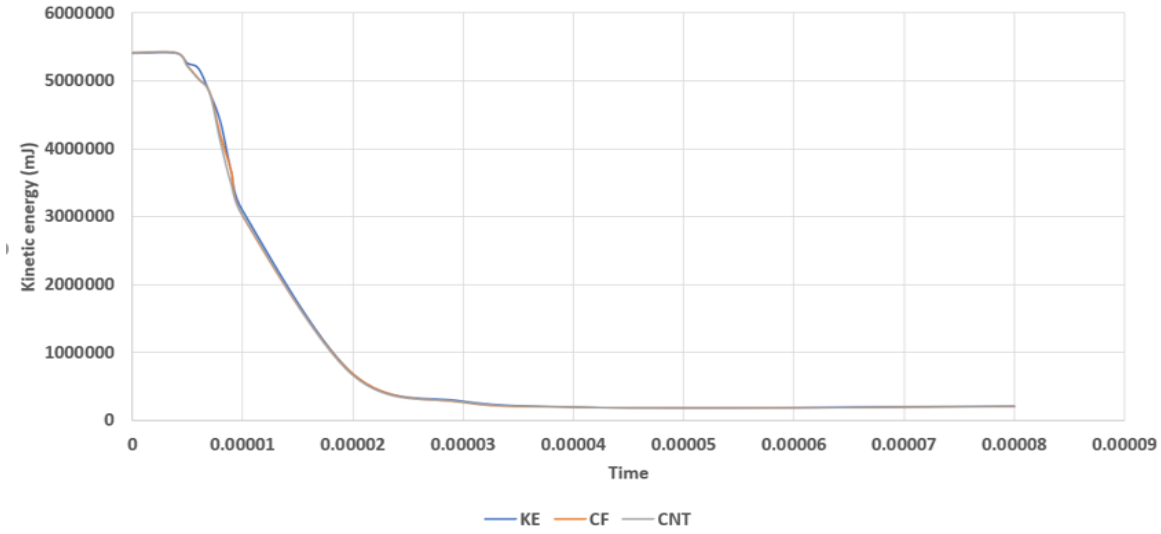

Figure 4. Kinetic energy plot for models with different skins at impact velocity 1400m/s

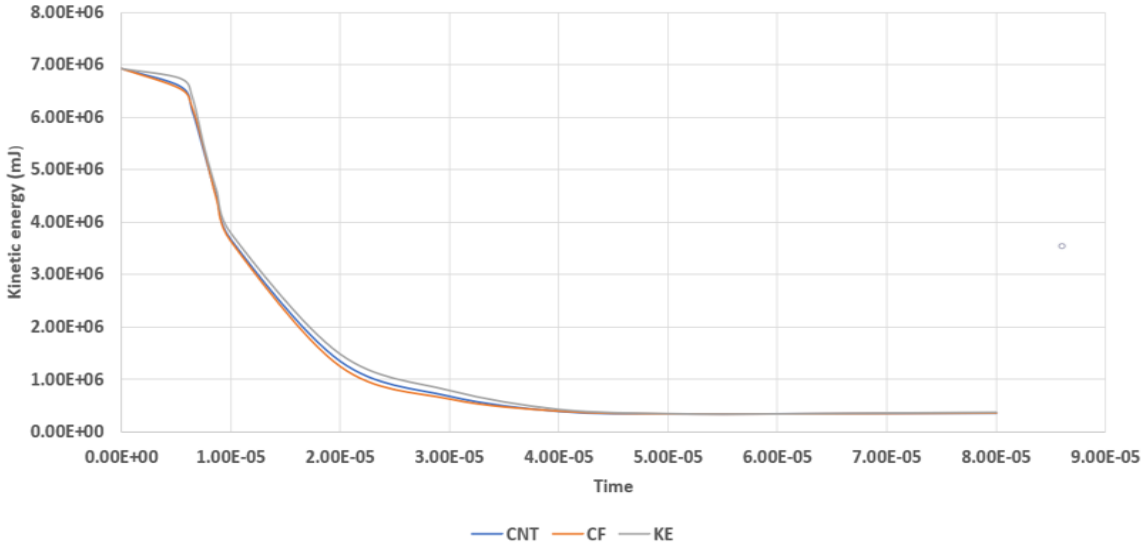

Figure 5. Kinetic energy plot for models with different skins at impact velocity 1600m/s

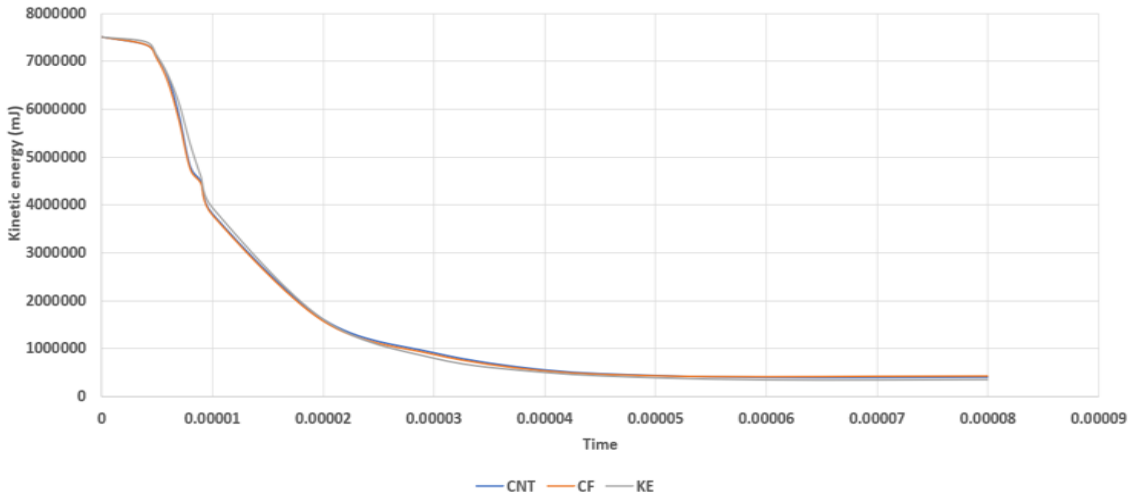

Figure 6. Kinetic energy plot for models with different skins at impact velocity 1700m/s

Figures 7, 8, 9 and 10 show the stages of penetration of projectile at step 0,1,2,3 and 4 through the sandwich armor with Carbon/Epoxy (T300 6k/ Epon 862) skins at 1600m/s. The sandwich armor with different skin compositions and a relative thickness of 3mm for each top and bottom skins, were simulated with an impact velocity of 1700m/s. A comparison of energy absorption and residual velocities of the combination of models are performed.

It was seen that all combination of sandwich armors with different skin composition of 3mm thickness demonstrated complete penetration. Among the simulated combination of model, the sandwich armor with Kevlar29/epoxy as skin had the highest residual velocity, signifying least energy absorption. However, sandwich armor with Carbon/Epoxy (T300 6k/ Epon 862) and Carbon/Epoxy (T300 6k/ Epon 862, with 4% carbon nanotube) as skins, had energy absorption and residual velocities relatively close. A closer review showed that, carbon/epoxy with reinforced carbon nanotubes had the least residual velocity and the highest energy absorption value.

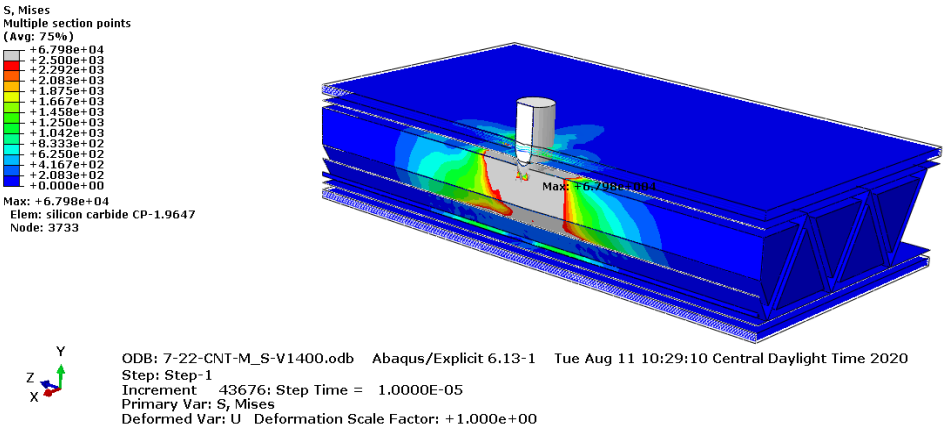

Figure 7. Cut sectional view of sandwich armor with Carbon/Epoxy (T300 6k/ Epon 862) skins subjected to impact velocity 1600m/s at step 1

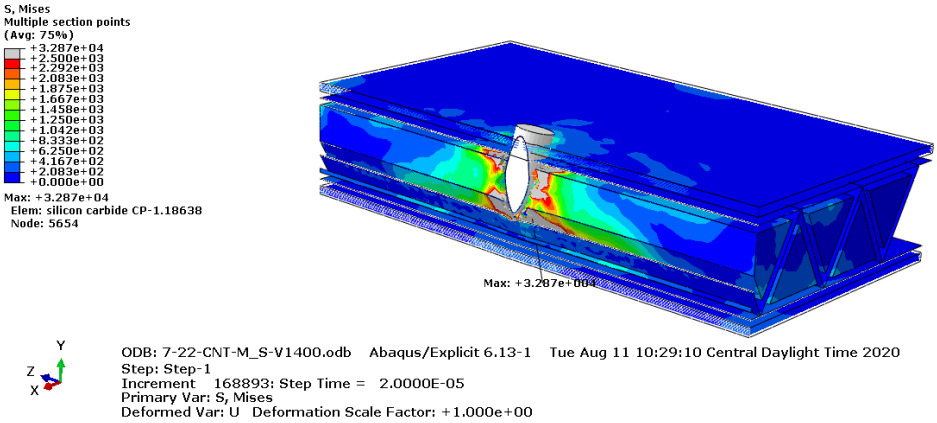

Figure 8. Cut sectional view of sandwich armor with Carbon/Epoxy (T300 6k/ Epon 862) skins subjected to impact V1600m/s at step 2

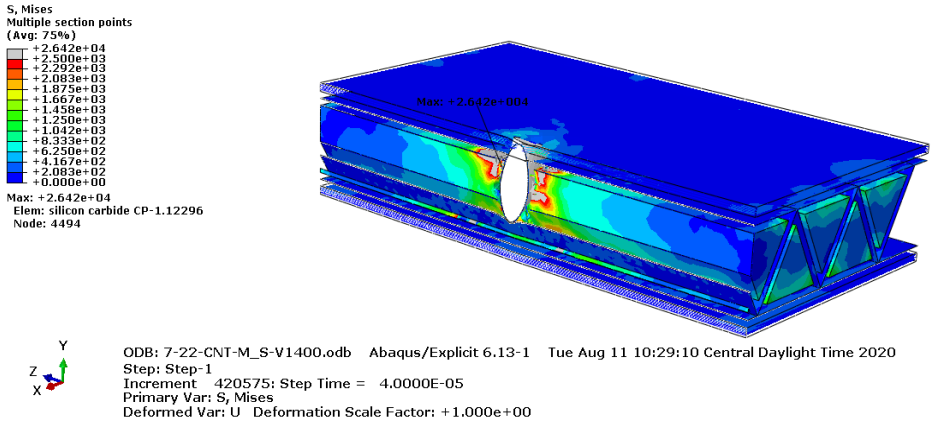

Figure 9. Cut sectional view of sandwich armor with Carbon/Epoxy (T300 6k/ Epon 862) skins subjected to impact V1600m/s at step 3

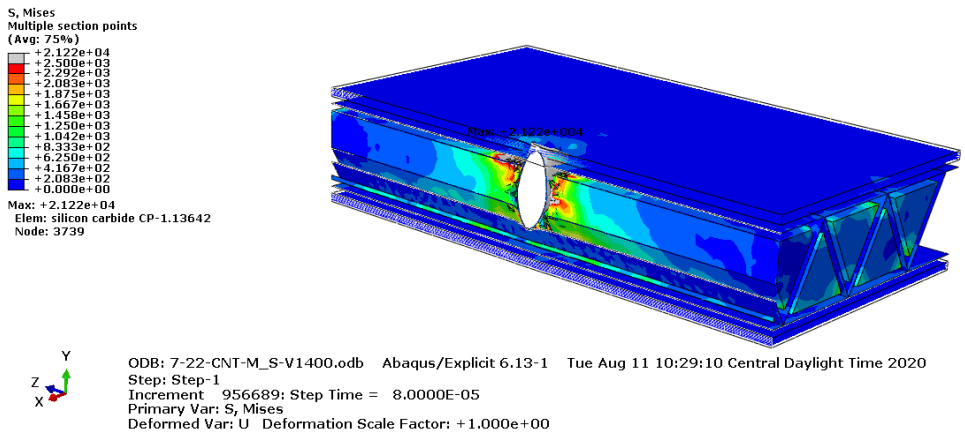

Figure 10. Cut sectional view of sandwich armor with Carbon/Epoxy (T300 6k/ Epon 862) skins subjected to impact V1600m/s at step 4

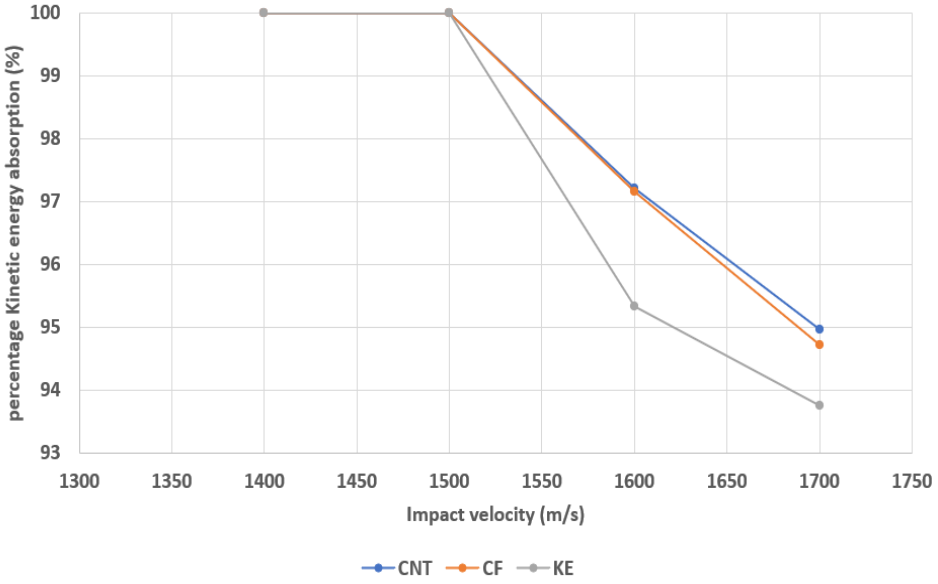

Figure 11. Percentage energy absorption of sandwich armors with 2mm skin at different impact velocities

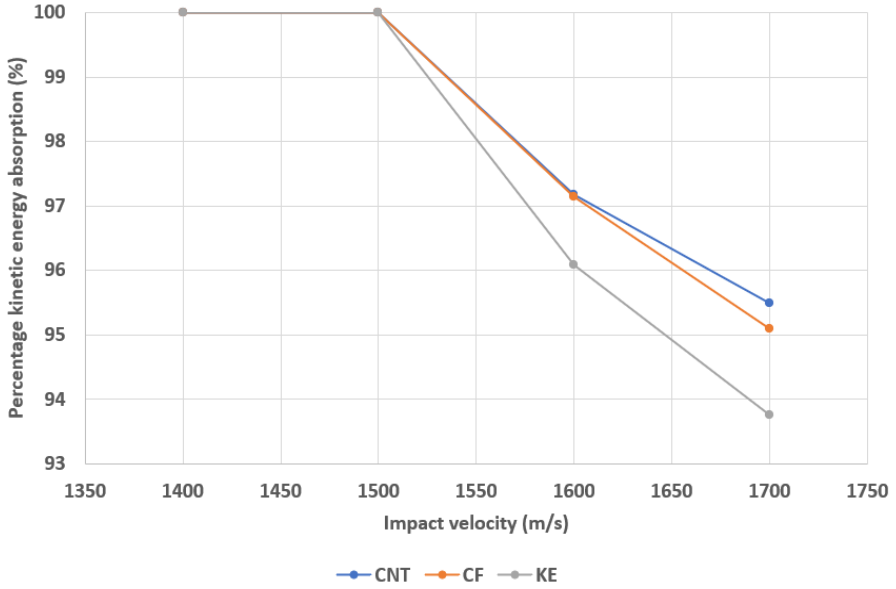

Figure 12. Percentage energy absorption of sandwich armors with varied skins with 3 mm thickness at different impact velocities

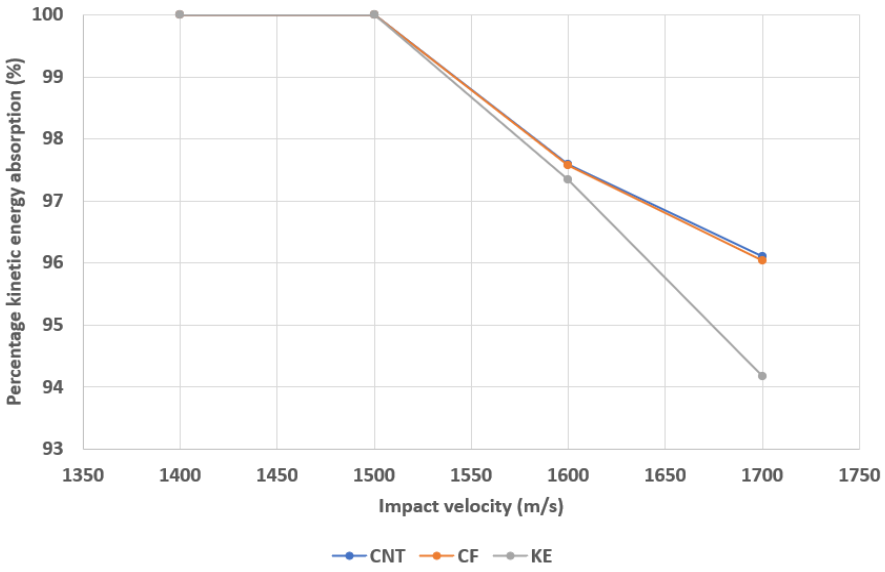

Figure 13. Percentage energy absorption of sandwich armors with varied skins with 4 mm thickness at different impact velocities

3.1. Comparison of Energy Absorption

The energy absorption of different sandwich armors with varied skins were simulated at velocities 1400m/s, 1500m/s, 1600m/s and 1700m/s where significant penetration in the armor is noticed. The energy absorption of each model varies considerably with respect to time. Energy absorption can be calculated using the following equation

$$Energy\ absorption = \frac{1}{2}.m.(v_i^2 - v_f^2)$$

m = Mass of the projectile, v_i = Initial velocity, v_f = Final velocity

Figure 11 shows the plot for percentage energy absorption of sandwich armors with kevlar 29/ phenolic matrix, carbon fiber/epoxy (T300 6k/ Epon 862) and carbon fiber/epoxy (T300 6k/ Epon 862, with 4% carbon nanotube) as skins. At velocities 1400 m/s and 1500 m/s as there is no penetration seen the kinetic energy absorption is equal to 100%. At velocity 1600 m/s and 1700 m/s there is significant penetration seen and the projectile exited with a residual velocity, which is not absorbed by the sandwich structure.

The results obtained from the simulation of sandwich armors with 3 mm skin thickness impacted at different velocities are compared using the kinetic energy absorption. Figure 12 shows the percentage kinetic energy absorption versus impact velocity plot for 3 mm skins. It is observed that the percentage of kinetic energy absorption increases from 2 mm to 3 mm skin.

Figure 13 shows the percentage of kinetic energy absorption versus impact velocity plot for 4 mm skins. It is seen that the energy absorption is 100% at impact velocities 1400 m/s and 1500 m/s as there is no penetration of the sandwich structure is seen. However, there is penetration of the sandwich models at impact velocities 1600 m/s and 1700 m/s.

Table 1 outlines the impact behavior of sandwich armors with varied parameters. The parametric change like skin composition, skin thickness and impact velocities have major influence on the performance of the armor, which is measured in terms of energy absorption and residual energy. The sandwich armor combination is varied with skin composition made of kevlar 29/phenolic matrix, carbon fiber/epoxy (T300 6k/ Epon 862) and carbon fiber/epoxy (T300 6k/ Epon 862, with 4% carbon nanotube) with a relative thickness of 2 mm, 3 mm and 4 mm. The impact velocities for the series of models with 2 mm, 3 mm and 4 mm thick skins are carried out at 1400 m/s, 1500 m/s, 1600 m/s and 1700 m/s. The table contains the tabulation of numeric analysis results like residual velocity and energy absorption. The tabulated results from the numeric analysis serve as an overview for ballistic performance of different sandwich armors. Using this table and results the choice for best combination of armor will be selected by reviewing the tabulated results.

3.2. Validation

The sandwich composite armor model used in the research is unique in-terms skin composition, combination of materials, geometry and assembly. There is no experimental data available in the literature which aligns with the current model in the research. Due to limitations of manufacturing and testing facilities of the sandwich composite armor, a kevlar/epoxy laminate finite element model is validated with the experimental test results found in the literature and also an inhouse testing result. In this section the validation of finite element model using the experimental test result found in the literature is discussed.

Experimental data pertaining to impact testing of kevlar/epoxy laminate is found in literature [28]. A similar model is developed in Abaqus, closely following the material properties, assembly and dimensions as mentioned in the literature. This model developed for validation purpose is simulated in Abaqus with same impact velocities

as mentioned in the experimental procedure and the results are compared. The Johnson cook damage parameters for the aluminum plate is found in [29] are used in the validation model.

Table 1. Ballistic performance of sandwich armors with varied composite skin composition and different velocity

Material	Skin thickness (mm)	Initial velocity (m/s)	Residual velocity (m/s)	% Energy absorbed
Kevlar 29/phenolic matrix + triangular corrugated (Al7039) core + silicon carbide prismatic centerpiece block + kevlar 29/ phenolic matrix	2	1400	0	100
	2	1500	0	100
	2	1600	345.654	95.33
	2	1700	426.77	93.69
	3	1400	0	100
	3	1500	0	100
	3	1600	316.67	96.08
	3	1700	424.32	93.76
	4	1400	0	100
	4	1500	0	100
	4	1600	260.24	97.35
	4	1700	410.28	94.17
Carbon fiber/epoxy (T300 6k/ Epon 862) + triangular corrugated (Al7039) core + silicon carbide prismatic centerpiece block + carbon fiber/epoxy (T300 6k/ Epon 862)	2	1400	0	100
	2	1500	0	100
	2	1600	270.08	97.15
	2	1700	390.27	94.72

Table 1. Continued

Material	Skin thickness (mm)	Initial velocity (m/s)	Residual velocity (m/s)	% Energy absorbed
Carbon fiber/epoxy (T300 6k/ Epon 862) + triangular corrugated (Al7039) core + silicon carbide prismatic centerpiece block + carbon fiber/epoxy (T300 6k/ Epon 862)	3	1400	0	100
	3	1500	0	100
	3	1600	270.08	97.16
	3	1700	376.29	95.10
	4	1400	0	100
	4	1500	0	100
	4	1600	260.24	97.35
	4	1700	338.36	96.03
Carbon fiber/epoxy (T300 6k/ Epon 862, with 4% carbon nanotube) + triangular corrugated (Al7039) core + silicon carbide prismatic centerpiece block + carbon fiber/epoxy (T300 6k/ Epon 862, with 4% carbon nanotube)	2	1400	0	100
	2	1500	0	100
	2	1600	267.00	97.21
	2	1700	381.19	94.97
	3	1400	0	100
	3	1500	0	100

Table 1. Continued

Material	Skin thickness (mm)	Initial velocity (m/s)	Residual velocity (m/s)	Energy absorbed (J)	% Energy absorbed
Carbon fiber/epoxy (T300 6k/ Epon 862, with 4% carbon nanotube) + triangular corrugated (Al7039) core + silicon carbide prismatic centerpiece block + carbon fiber/epoxy (T300 6k/ Epon 862, with 4% carbon nanotube)	3	1600	268.91	6940.64	97.17
	3	1700	360.87	7699.76	95.49
	4	1400	0	5369.46	100
	4	1500	0	6149.48	100
	4	1600	248.45	6970.17	97.59
	4	1700	334.86	7750.24	96.11

Table 2. Comparison of experimental data with simulation data [34]

Initial velocity (m/s)	Energy absorbed		Difference between experimental and numerical data (%)
	Experimental (J)	Simulation (J)	
180	70.11	80.67	13.09%
210	90.89	109.80	17.22%
240	108.59	114.03	4.77%

Table 2 shows the comparison between experimental values and numerical analysis values from the simulation. The deviation may be due to the velocity reading error in the experiment, the variation of material properties and failure criteria values used in the simulation. Some material properties are given in [28] and other required properties for simulation are used from another literature [29].

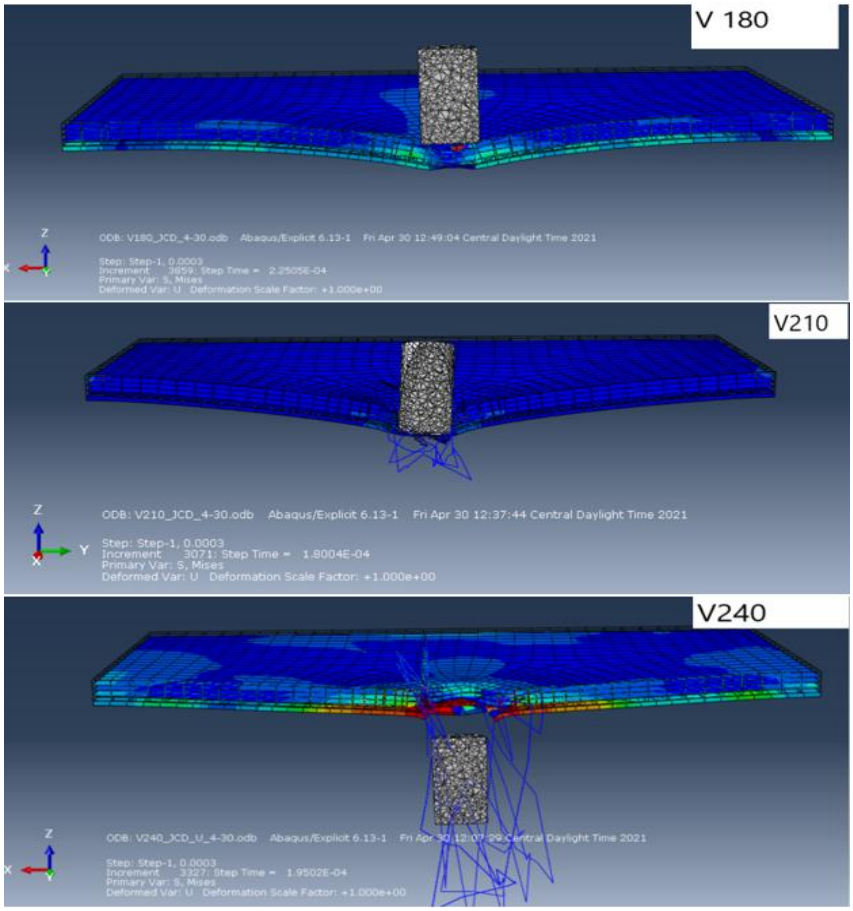

Figure 14. Stress contour of the validation model at three different impact velocities of 180 m/s, 210 m/s and 240 m/s, respectively

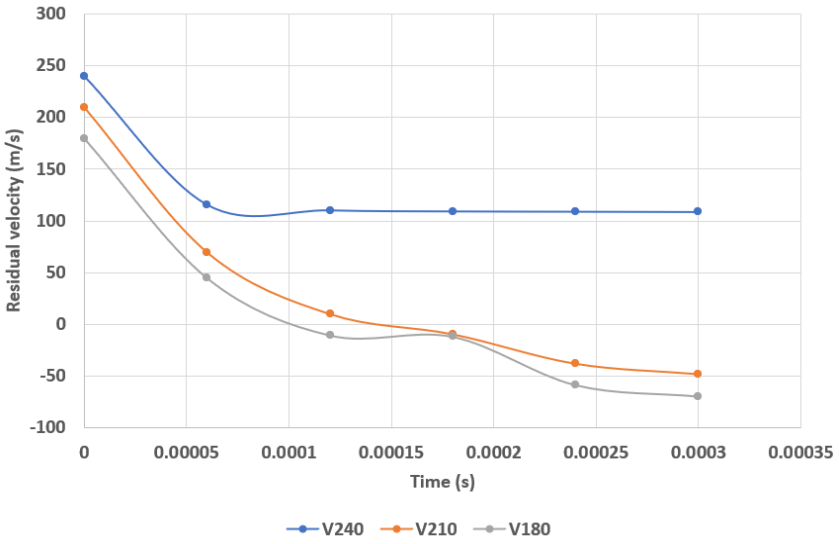

Figure 15. Residual velocity at V180 m/s, V210 m/s and V240 m/s

Figure 14 shows the stress contour plot of the validation model at three different velocities. At 180m/s, the projectile partial penetrated, at 210m/s the projectile fully penetrated and at 240m/s it fully penetrated.

Figure 15 shows the comparison of residual velocity plots of validation model simulated at V180 m/s, V210 m/s and V240 m/s. At 180m/s, the projectile absorbed about 80.67J, at 210m/s the projectile absorbed about 109.80J and at 240m/s it absorbed about 114.03J. The maximum deviation from experimental was found about 17.22%.

4. Conclusions

The impact analysis carried out on the sandwich armor in the research are made of composite skins at the top and bottom, along with a low-density core in between the skins. The composite skins used in this research are made of kevlar 29/phenolic matrix, carbon fiber/epoxy (T300 6k/ Epon 862) and carbon fiber/epoxy (T300 6k/ Epon 862, with 4% carbon nanotube) cross-ply weave. Three sets of models are created using a variation of skin materials with one set of models with 2 mm skin thickness, the other with 3 mm skin thickness and the third set with 4 mm skin thickness. The core is made of ceramic prismatic blocks called as centerpiece which are made of silicon carbide. These silicon carbide centerpieces serve as individual insertion, collectively making up the core. The individually inserted prismatic blocks of silicon carbide centerpiece are held in place and together by a triangular profile corrugated structure made of Al 7039. The corrugated Al 7039 structure housing the individual silicon carbide centerpiece together make the core. The core integrated with top and bottom skins made of composite materials together accounts for the sandwich armor, which is studied by impacting the armor with a projectile made of hardened steel at different impact velocities.

The sandwich armor is simulated at different velocities starting from 1400 m/s, 1500 m/s, 1600 m/s and 1700 m/s for models with skin thickness of 2 mm, 3 mm and 4 mm. It is noticed that the residual velocity of sandwich armors increased with increase in impact velocity. At relatively low impact velocity all combination of sandwich armors demonstrated energy absorption close to 100% with low residual velocities. With increase in impact velocity, there is a significant increase in the magnitude of kinetic energy absorbed and an increase in the residual velocity. However, there is complete penetration and perforation of all models of sandwich armors at impact velocities of 1600 m/s and higher. At high velocities, the projectile is seen to penetrate completely and exit with a residual velocity, which is significantly lower than the impact velocity, as the armor has successfully absorbed a large portion of energy before damage.

After performing a series of simulation with different model configuration and impact velocities, the results from the simulation are tabulated in terms of energy absorption and residual velocities, which serves as a bird's eye view into the performance and characteristic behavior of different sandwich armors under consideration. The behavior is almost similar to all models at low velocity, but there is a considerable difference in terms of energy absorption and residual velocity. The percentage difference in energy absorption and residual velocity among the models increased with the increase in impact velocity. It is observed that the sandwich armors with carbon fiber/epoxy (T300 6k/ Epon 862, with 4% carbon nanotube) as skins showed higher energy absorption and lower values of residual velocity, whereas the models with kevlar 29/phenolic matrix as skins yielded the least values of energy absorption and higher values of residual velocity at all thickness and velocity variants.

The accuracy of the simulation is validated by comparing the results from the experimental data obtained from a literature and by comparing the results obtained from the experimental data obtained from the impact test performed on a kevlar panel. The results variation is observed and the reasons for variations are explained.

ACKNOWLEDGEMENTS

This work is supported by the Army Research Office (ARO) Grant Award Number W911NF-18-1-0478.

Conflict of Interest

The authors declare that they have no known competing financial interests or personal relationships that could have appeared to influence the work reported in this paper.

REFERENCES

[1] A. A. Ramadhan, A. A. Talib, A. M. Rafie, R. Zahari, The Influence of Impact on Composite Armour System Kevlar-29/polyester-Al2O3, IOP Conference Series: Materials Science and Engineering, vol. 36, no. 1, pp. 1-14, 2012.

[2] F. Elaldi, Multilayer Ceramic Composite Armor Design and Impact Tests, 37th Int'l Conf & Expo on Advanced Ceramics & Composites, vol. 34, no. 2, pp. 173-8, 2013.

[3] X. Ma, X. Li, S. Li, R. Li, Z. Wang, G. Wu, Blast response of Gradient Honeycomb Sandwich Panels with Basalt Fiber Metal Laminates as Skins, International Journal of Impact Engineering, vol. 123, pp. 126-139, 2019.

[4] D. Q. Hu, J. R. Wang, L. K. Yin, Z. G. Chen, R. C. Yi, & C. H. Lu, Experimental Study on the Penetration Effect of Ceramics Composite Projectile on Ceramic/A3 Steel Compound Targets, Defense Technology, vol. 13, no. 4, pp. 281-287, 2017.

[5] A.R. Bhat, Honeycomb in Hybrid Composite Armor Resisting Dynamic Impact, PhD diss., Mechanical and

Aerospace Eng., Oklahoma State University, 2015. https://shareok.org/bitstream/handle/11244/299565/Bhat_okstate_0664D_14211.pdf?sequence=1&isAllowed=y (accessed 13 August 2019).

[6] E. Randjbaran, R. Zahari, N. A. Abdul Jalil, D. L. Abang Abdul Majid, Hybrid Composite Laminates Reinforced with Kevlar/Carbon/Glass Woven Fabrics for Ballistic Impact Testing, The Scientific World Journal, vol. 2014, pp. 1-7, 2014.

[7] Y. Pekbey, K. Aslantaş, N. Yumak, Ballistic Impact Response of Kevlar Composites with Filled Epoxy Matrix, Steel and Composite Structures, vol. 22, no. 4, pp.191-200, 2017.

[8] A. B. H. D. S. Figueiredo, É. P. Lima Júnior, A. V. Gomes, G. B. M. D. Melo, S. N. Monteiro, R. S. D. Biasi, Response to Ballistic Impact of Alumina-UHMWPE Composites, Materials Research, vol. 21, no. 5, pp. 1-5, 2018.

[9] M. R. O'Masta, B. P. Russell, V. S. Deshpande, An exploration of the Ballistic Resistance of Multilayer Graphene Polymer Composites, Extreme Mechanics Letters, vol. 11, pp. 49-58, 2017.

[10] K. Akella, N. K. Naik, Composite armour—A Review, Journal of the Indian Institute of Science, vol. 95, no. 3, pp. 297-312, 2015.

[11] Y. Pekbey, K. Aslantaş, N. Yumak, Ballistic Impact Response of Kevlar Composites with Filled Epoxy Matrix, Steel and Composite Structures, vol. 22, no. 4, pp.191-200, 2017.

[12] D. Q. Hu, J. R. Wang, L. K. Yin, Z. G. Chen, R. C. Yi, & C. H. Lu, Experimental Study on the Penetration Effect of Ceramics Composite Projectile on Ceramic/A3 Steel Compound Targets, Defense Technology, vol. 13, no. 4, pp. 281-287, 2017.

[13] A. B. H. D. S. Figueiredo, É. P. Lima Júnior, A. V. Gomes, G. B. M. D. Melo, S. N. Monteiro, R. S. D. Biasi, Response to Ballistic Impact of Alumina-UHMWPE Composites, Materials Research, vol. 21, no. 5, pp. 1-5, 2018.

[14] K. Xia, H. Zhan, D. A. Hu, Y. Gu, Failure Mechanism of Monolayer Graphene under Hypervelocity Impact of Spherical Projectile, Scientific reports, vol. 6, no. 1, pp. 1-10, 2016.

[15] A. Tasdemirci, G. Tunusoglu, Experimental and Numerical Investigation of the Effect of Interlayer on the Damage Formation in a Ceramic/Composite Armor at a Low Projectile Velocity, Journal of Thermoplastic Composite Materials, vol. 30, no. 1, pp. 88-106, 2017.

[16] E. L. Fasanella, R. L. Boitnott, S. Kellas, Test and Analysis Correlation of High Speed Impacts of Ice Cylinders, In Proceedings from 9th International LS-DYNA Users Conference, pp. 1-12, 2006.

[17] M. R. O'Masta, B. P. Russell, V. S. Deshpande, An exploration of the Ballistic Resistance of Multilayer Graphene Polymer Composites, Extreme Mechanics Letters, vol. 11, pp. 49-58, 2017.

[18] M. Rodríguez Millán, C. E. Moreno, M. Marco, C. Santiuste, H. Miguélez, Numerical Analysis of the Ballistic Behavior of Kevlar® Composite under Impact of Double-Nosed Stepped Cylindrical Projectiles, Journal of reinforced plastics and composites, vol. 35, no. 2, pp. 124-137, 2016.

[19] M. Tarfaoui, A. El Moumen, K. Lafdi, Progressive Damage Modeling in Carbon Fibers/Carbon Nanotubes Reinforced Polymer Composites, Composites Part B: Engineering, vol. 112, pp. 185-195, 2017.

[20] M. N. Saquib, Ballistic Impact on a Sandwich-Structured Composite Armor, MS thesis, Mechanical and Industrial Eng., Texas A&M University-Kingsville, 2019.

[21] S. Alam, B. Adegbesan, D. Khanal, Ballistic Performance of Sandwich Composite Armor System, International Journal of Composite Materials 2020, 10(2): 40-49.

[22] G. Guo, S. Alam and L. Peel, Advanced Hybrid Composite Armors for Ballistic Impact, Composite part C: 3 (2020) 100061.

[23] I. Lapczyk, J. A. Hurtado, Progressive Damage Modeling in Fiber-Reinforced Materials, Composites Part A: Applied Science and Manufacturing, vol. 38, no. 11, pp. 2333-2341, 2007.

[24] Matweb, Aluminum 7039 Properties. http://www.matweb.com/search/datasheet_print.aspx?matguid=e4e262e692284ac994651fe1e268322c (accessed 25 March 2020).

[25] Msstate, Damage Data for Aluminum 7039.https://icme.hpc.msstate.edu/mediawiki/images/f/f2/S1R8N3_A1_DMG.data.txt (accessed 6 April 2020).

[26] High Velocity Impact of a Ceramic Target, Example Problem 2.1.18, v 6.14, Dassault Systems, 2014. http://130.149.89.49:2080/v6.14/pdf_books/CAE.pdf (accessed 6 April 2020).

[27] Eroding Projectile Impacting Eroding Plate, Example Problem 2.1.4, v 6.14, Dassault Systems, 2016. http://130.149.89.49:2080/v2016/pdf_books/EXAMPLES_1.pdf (accessed 11 April 2020).

[28] A. A. Ramadhan, A. A. Talib, A. M. Rafie, R. Zahari, High Velocity Impact Response of Kevlar-29/Epoxy and 6061-T6 Aluminum Laminated Panels, Materials & Design, vol. 43, pp. 307-321, 2013.

[29] J. Fish, C. Oskay, R. Fan, R. Barsoum, Al 6061-T6-Elastomer Impact Simulations, Electronic document, 2005. https://www.scorec.rpi.edu/REPORTS/2005-11.pdf (accessed 28 April 2021).